Chapter 9

Gold Nanorod Array Biochip for Label-Free, Multiplexed Biological Detection

Zhong Mei, Yanyan Wang, and Liang Tang

Abstract

Gold nanorod (GNR) based label-free sensing has been attractive due to its unique property of localized surface plasmon resonance (LSPR). Compared to bulk gold, the SPR of GNRs is more sensitive to the refractive index change caused by biological binding in the close proximity. Numerous studies have reported biological detection in solution based GNR probes. However, the biosensing has the intrinsic problems of fluctuating readings and short storage time due to nanoparticle aggregation. In contrast, a chip-based nanorod biosensor is a more robust and reliable platform. We have developed a nanoplasmonic biosensor in a chip format by immobilizing functionalized GNRs on a (3-mercaptopropyl)trimethoxysilane modified glass substrate. The covalent Au-S bond ensures a strong GNR deposition on the substrate. This biochip exhibits a high sensitivity and stability when exposed to physiological buffer with high ionic strength. Another advantage of GNR as optical transducer is its LSPR peak dependence on the aspect ratio, which provides an ideal multiplexed detection mechanism. GNRs of different sizes that exhibit distinct SPR peaks are combined and deposited on designated spots of a glass substrate. The spectral shift of the respective peaks upon the biological binding are monitored for simultaneous detection of specific analytes. Coupled with a microplate reader, this spatially resolved GNR array biochip results in a high-throughput assay of samples as well as multiplexed detection in each sample. Since most biological molecules such as antibodies and DNA can be linked to GNR using previously reported surface chemistry protocol, the label-free nanosensor demonstrated here is an effective tool for protein/DNA array analysis, especially for detection of disease biomarkers.

Key words Gold nanorods, Surface plasmon resonance, Biochip, Multiplex

1 Introduction

When the dimension of a matter is reduced to the nanometer scale (1–100 nm), the material can exhibit distinct properties from its bulk form, including optical, structural, electrical, and chemical properties. These changes make nanoparticles promising for a wide range of biomedical applications such as biosensing, imaging, and drug delivery [1–3]. Among diverse nanomatrials, plasmonic nanoparticles (Au, Ag) are attractive because of their unique optical

Avraham Rasooly and Ben Prickril (eds.), *Biosensors and Biodetection: Methods and Protocols Volume 1: Optical-Based Detectors*, Methods in Molecular Biology, vol. 1571, DOI 10.1007/978-1-4939-6848-0_9,

property, surface plasmon resonance (SPR) which arises from free electron oscillation induced by electromagnetic radiation (i.e., light) [4]. The SPR results in a strong absorption of the incident light at specific wavelength region which can be measured by a UV–Vis spectrophotometer. The SPR band intensity and wavelength depends on the metal type, particle size, shape, composition, and the dielectric constant of the surrounding medium, as theoretically depicted by Mie theory [5]. For a given nanosphere, the SPR condition is $\varepsilon_r = -2\varepsilon_m$, where ε_r is the dielectric function of the metal, and ε_m is the dielectric constant of the medium. This indicates an increase in ε_m requires an increase in ε_r to satisfy the SPR condition. Practically, when the refractive index (n) of the surrounding medium increases, the extinction spectrum shifts to longer wavelengths (known as red-shift). Since most biomolecules ($n \approx 1.4$–1.45) have a higher refractive index than water ($n \approx 1.33$), a red shift of the SPR peak is observed when the biomolecules are absorbed to the nanoparitlce surface in aqueous medium. If the nanoparticle is functionalized with special probe (i.e., antibody), the shifts can be induced by the specific target (i.e., antigen) binding to the probe. Thus, by monitoring the SPR shifts using UV–Vis spectrophotometer, biological events on the surface of plasmonic nanoparticles can be quantitatively detected. This is the mechanism of a label-free SPR biosensor.

Recently, gold nanoparticles (GNPs) have been widely used in biosensing because of their facile surface modification, chemical stability and excellent biocompatibility [6, 7]. GNPs with various shapes including nanosphere, nanarod, nanostar, nanoshell, and nanocage are reported for different sensing purposes [8]. Both theoretical study and experimental results have shown that nanorods have a greater performance than nanospheres, which is characterized by the sensitivity (i.e., plasmon peak shift per unit change in the effective refractive index of the surrounding medium, RIU^{-1}). Given its simple synthesis and large tunability of surface plasmon, gold nanorods (GNRs) have been a good alternative to other shapes in SPR-based biosensing [9]. Different from bulk gold films utilized in conventional SPR techniques, the anisotropic shape and nanosize effect enable gold nanorods an extremely intensified local electromagnetic field along its longitudinal direction, which is highly sensitive to changes in the local refractive index [10]. Once biological events occur at the surface of GNRs, the change in the local refractive index will cause a longitudinal peak shift of the extinction spectra of GNRs, which can be measured by a UV–Vis spectrophotometer. Compared to the instrumental setup in traditional SPR techniques [11], this nanosensing method is more sensitive [12], user-friendly, and cost-effective.

In addition, the longitudinal SPR wavelength of GNR is tunable in a broad range from UV–visible to far infra-red region by varying its aspect ratio (length to width ratio). With advance in the

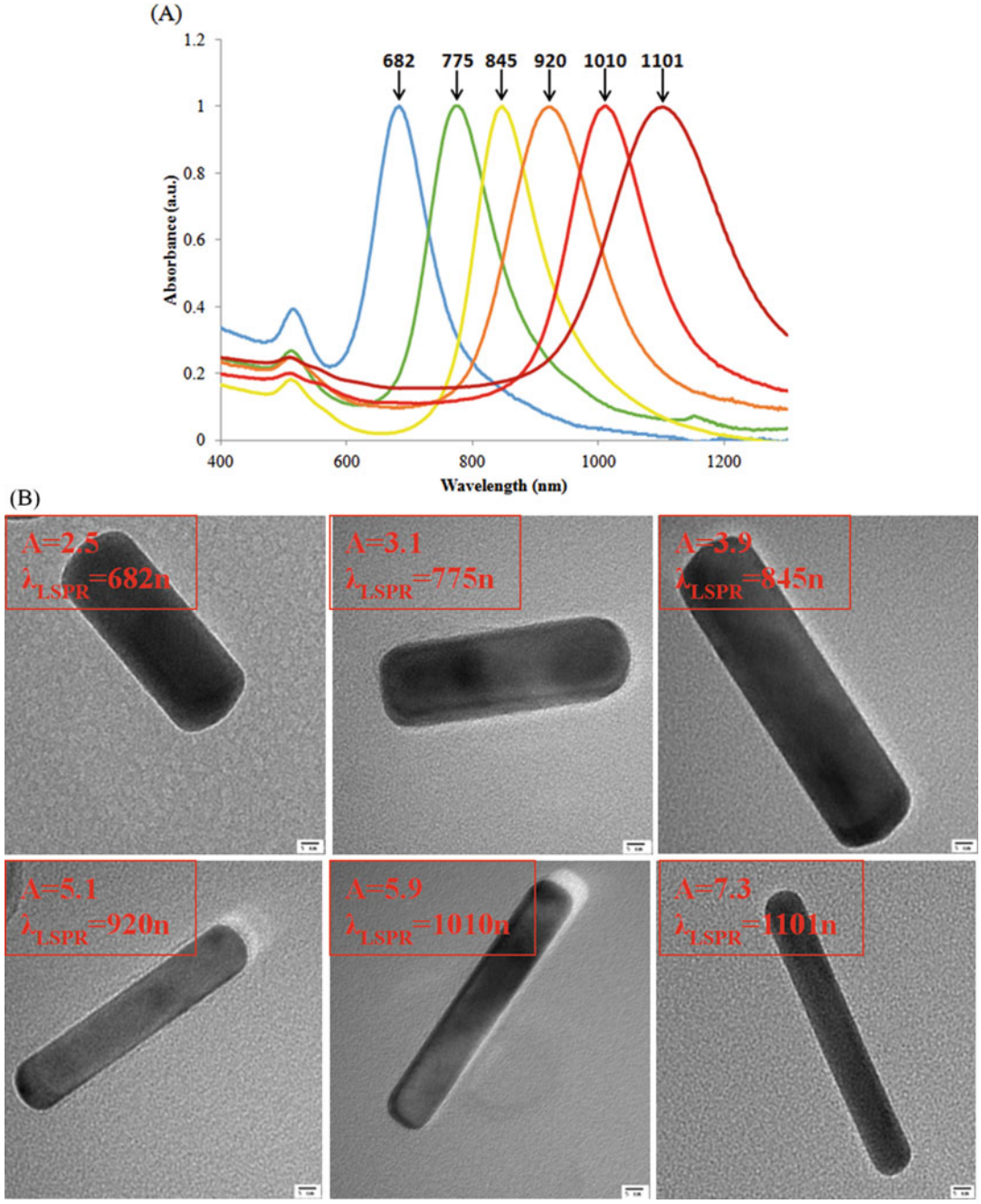

Fig. 1 (**a**) UV–Vis spectra of synthesized GNRs; (**b**) TEM images of GNRs. The longitudinal plasmon peak is tunable by varying rod aspect ratio

seed-mediated growth approach [13, 14], high-quality GNR can be synthesized with precise control of the size and shape. Figure 1 shows the extinction spectra of six GNRs and their respective aspect ratios. As the nanorod size increases, the longitudinal plasmon peak

exhibits proportional red shifts. The correlation between aspect ratio (A) and the longitudinal SPR peak (λ_{LSPR}/nm) can be expressed as follows

$$\lambda_{LSPR} = 84.4A + 497.8 \quad (1)$$

This unique property facilitates a multiplexed biosensing. GNRs of different aspect ratios can be mixed to fabricate multiplexed bioprobes to detect specific analytes simultaneously. For example, if one sample contains two different antigens (antigen 1 and 2) to be detected/quantified simultaneously, GNR 1 (AR = 2.5, LSPR λ = 682 nm) can be functionalized with antibody 1 for antigen 1 detection while GNR 2 (AR = 5.1, LSPR λ = 920 nm) is functionalized with antibody 2. These two functionalized GNRs are then mixed and there will distinct plasmon bands for the specific GNR on the absorption spectrum. The first peak at ~520 nm represents the characteristic gold resonance in transverse direction which is less sensitive to local refractive index changes. The second peak at 682 nm and the third peak at 920 nm reflect the longitudinal peaks from GNR1 and GNR2, respectively. These two dominate peaks are distinctly separated, thereby enabling a simultaneous monitoring of plasmonic shift at both positions independently for the dedicated target antigen detection in a single sample. However, solution-based GNR probe has its intrinsic problems. First, multiple washes cannot be avoided in the process of fabricating GNR bioprobes. These cause extinction intensity change and fluctuate readings. Second, the stability of a GNR suspension depends on temperature and surfactant concentration, which results in short storage time of the GNR probes. As such, it is highly desired to develop a GNR nanosensor in a chip format which significantly strengthen the utility of this label-free biosensing modality as a powerful bioanalytical device [15].

Given that antibodies have primary amine group, it is feasible to chemically modify antibody molecules with thiolation reagent to enable gold–antibody linkage [16]. Thus, these GNR-conjugated antibodies can work as biological receptors or bioprobes for detecting specific antigens. Since many antibodies or antigens are disease-representing biomarkers, rapid detection with a low-cost, specific and sensitive biosensor is of great significance for clinical diagnosis. Therefore, we develop a chip-based GNR biosensor for antigen detection and then we extend this biochip into an array format, which enables high-throughput screening as well as multiplexed detection. Figure 2 is a schematic of three processes involved in a label-free, multiplexed LSPR biochip. Human IgG and rabbit IgG were used as a general analyte for demonstration. First, GNRs of varying sizes are functionalized with anti-human IgG and anti-rabbit IgG, respectively. Next, the functional GNRs are immobilized to a thiolated glass substrate to construct chip-based LSPR

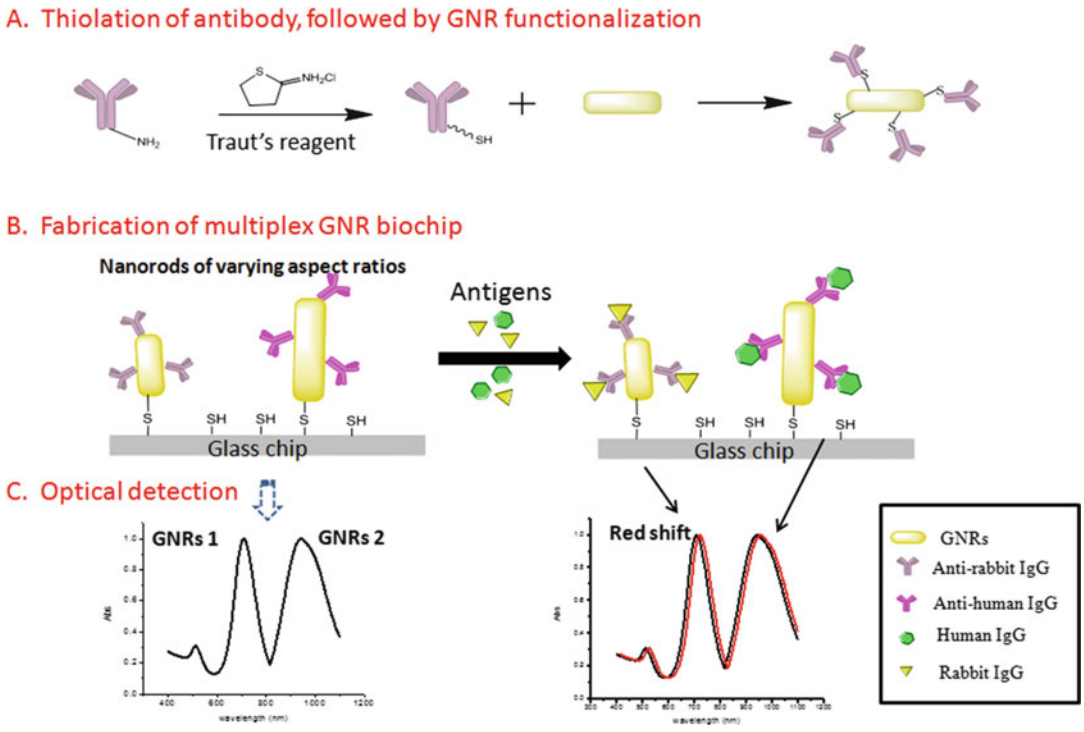

Fig. 2 Schematic of GNR biofunctionalization and design of label-free, multiplexed biosensing by GNRs of different aspect ratios. (**a**) Thiolation of antibody, followed by GNR functionalization. (**b**) Fabrication of multiplex GNR biochip. (**c**) Optical detection

sensor. When the antigens (human IgG and rabbit IgG) are present in the test samples, they will specifically bind to their respective antibodies (i.e., anti-human IgG and anti-rabbit IgG). Upon this binding, pronounced red shifts at the respective dominate LSPR bands are monitored by UV–Vis absorbance measurements. The magnitude of the red shift in the distinct LSPR peak wavelength is directly proportional to the amount of antigen binding onto the GNR probes.

2 Materials

2.1 Chemicals (See Note 1)

1. Gold(III) chloride trihydrate ($HAuCl_4$: 99%).
2. Sodium borohydride ($NaBH_4$:99%).
3. L-ascorbic acid (AA: 99%).
4. Cetyltrimethylammoniumbromide (CTAB).
5. Sodium oleate (NaOL).
6. Silver nitrate ($AgNO_3$:99%).
7. (3-mercaptopropyl)trimethoxysilane (MPTMS).

8. Poly (ethylene glycol) methyl ether thiol (SH-PEG, Mw∼5000).
9. 2-iminothiolane hydrochloride (Traut's reagent: 98%).

2.2 Working Solutions

1. $HAuCl_4$ is dissolved in MilliQ water at 10 mM and stored at 4 °C in dark.
2. Bisurfactant solution: a mixture of 7.0 g CTAB and 1.237 g NaOL is added into 250 mL distilled water and sonicated at 50 °C for completely dissolving.
3. $NaBH_4$ is dissolved in ice-cold water at 10 mM before use.
4. Piranha solution: a 3:1 mixture of concentrated sulfuric acid (98%) and hydrogen peroxide (30%) solution.
5. Phosphate buffered saline (PBS, pH 7.4, 0.01 M) is prepared by dissolving one pouch of dry powder in 1 L deionized water.
6. Goat anti-human IgG and anti-rabbit IgG (2 mg/mL) are diluted at 10 μg/mL with PBS and stored at −20 °C before use.
7. Human serum IgG and rabbit serum IgG are dissolved at various concentrations (10, 20, 30, 40, 50, 60 nM) with PBS.

2.3 Instruments

1. Beckman-Coulter UV-NIR spectrophotometer (DU@720, Fullerton, CA).
2. BioTek Multi-Detection Microplate Reader (Synergy™ 2, Winooski, VT).
3. MilliQ@ Direct Water Purification System instruments (EMD Millipore Corporation, Germany).

3 Methods (All Procedures Are Performed at Room Temperature Unless Notified Otherwise)

3.1 Chip Based Nanoplasmonic Biosensing for Single Antigen

3.1.1 Preparation of Gold Nanorods

1. Gold seed solution is prepared by adding 0.025 mL of 10 mM $HAuCl_4$ into 1 mL of aqueous 0.1 M CTAB, followed by adding 1 mL of 10 mM fresh-made ice-cold $NaBH_4$. The resulting solution is incubated at 27 °C for 30 min.
2. To prepare gold growth solution, 4 mM $AgNO_3$ is added to 20 mL of bisurfactant solution. The mixture is kept undisturbed at 30 °C for 15 min. Then 10 mL $HAuCl_4$ is added, followed by 90 min of stirring. 12.1 M HCl and 100 uL AA (64 mM) is added.
3. A specific amount of the seed solution is added to the growth solution. The resulting mixture is incubated at 29 °C overnight for full nanorod growth. To synthesize nanorods of varying aspect ratios, the amount of $AgNO_3$, HCl and seed solution are adjusted following the recipe (*see* Table 1).

Table 1
Growth conditions for GNRs with respective longitudinal SPR wavelengths

$AgNO_3$ (mL)	HCl (μL)	Seed (μL)	λ_{LSPR} (nm)
0.6	120	32	630
1.44	120	32	775
1.92	120	32	840
1.92	140	64	950

4. The suspension is centrifuged twice at 8500 rpm for 30 min. 5 mL MilliQ water is then added to resuspend the solid pellets and centrifuged again at 13000 rpm for 3 min. The resulting pellets are then redispersed in 5 mL solution (*see* **Note 2**).

3.1.2 Fabrication of Nanoplasmonic Biochip

1. Microscopy glass slides (ITO-coated, 7 mm × 50 mm × 0.7 mm; Delta Technologies, Loveland, CO) are cleaned with the piranha solution and heated at 70 °C for 40 min (*see* **Note 3**).
2. Rinse the glass slides with distilled water, ethanol and dry with nitrogen gas.
3. Immerse the cleaned slides in a MPTMS (10% v/v in ethanol) solution.
4. After 2.5 h of incubation, the slides are thoroughly rinsed with ethanol, water and dried with nitrogen gas.
5. To functionalize GNRs with antibodies, 20 μL of Traut's reagents (5 mg/mL) are first added to 0.1 mL of anti-human IgG for 2 h [16]. Then 200 μL of GNR solution and 100 μL of SH-PEG (10 mg/mL) are added for incubation overnight (*see* **Note 4**).
6. The anti-IgG conjugated GNRs are separated from the excess antibody by centrifugation at 8000 rpm for 10 min and finally redispersed in PBS.
7. Immerse the MPTMS-treated glass in the functionalized GNR colloids. After 2 h of shaking at 700 rpm, the glass substrates are rinsed several times with water and dried with nitrogen gas (*see* **Note 5**) .

3.1.3 Antigen Detection

1. Position the GNR-modified glass chip into a UV cuvette (2.5 mL, 12.5 × 12.5 × 45 mm; BrandTech Scientific, Wertheim, Germany) and insert the cuvette to the cuvette holder of the Beckman-Coulter UV-NIR spectrophotometer, as shown in Fig. 3. Measure the UV–Vis absorption spectra of GNRs on glass as the baseline.

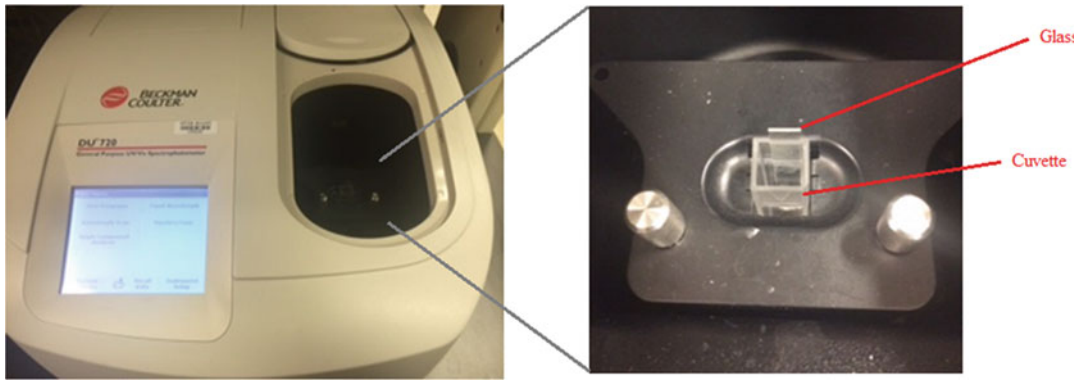

Fig. 3 Schematic of the measurement of UV–Vis spectrum using Beckman spectrophotometer

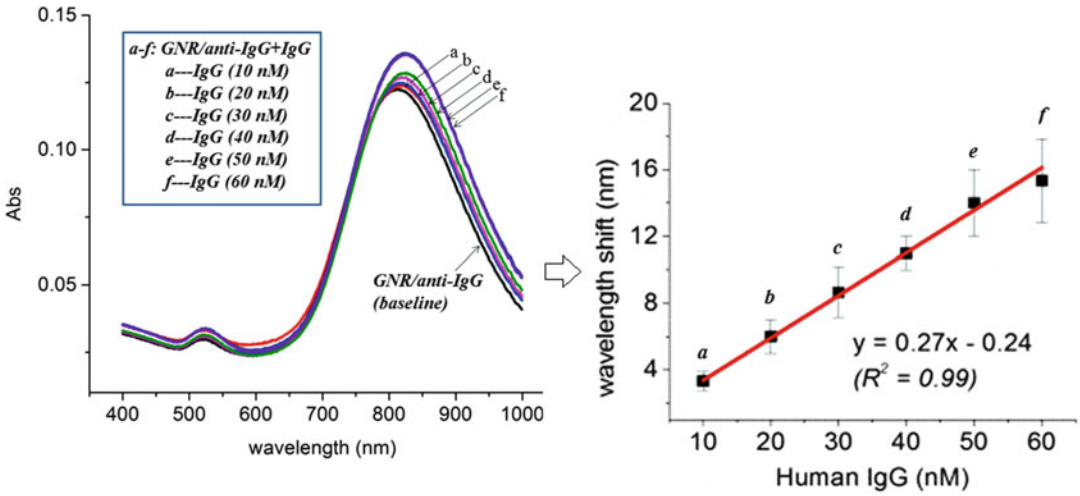

Fig. 4 Detection of human IgG targets by anti-human IgG modified GNRs biochip. The *black curve* is the absorption spectrum of anti-IgG modified GNRs biochip (baseline). The other six *colored curves* are absorptions spectra of the GNR/anti-IgG chip incubated in the target human IgG samples of varying concentrations (*a–f*: 10–60 nM). The peak wavelength at ~840 nm shows a red shift after IgG binding to the GNR/anti-IgG chip. A higher concentration of IgG resulted in a larger red shift. Calibration curve of the red-shift versus IgG concentration shows the longitudinal plasmon shift as a function of human IgG concentration

Dilute human IgG at a series of concentrations from 10 to 60 nM with PBS, then apply these samples on the GNR biochip surface and incubate for 30 min.

2. After washing the chips with water, the UV–Vis absorption spectra are measured again.
3. By comparing the spectra before and after human IgG conjugation, the red shift of longitudinal plasmon peak is observed in proportional to the target concentration (Fig. 4, *see* **Note 6**).

3.2 Nanoarray Based Multiplexed Biosensing for Multiple Antigens

The methods for gold nanorod synthesis and functionlization are similar as described above. To achieve multiplexed biosensing, GNRs with varying sizes are mixed and deposited on one substrate. Here, we take two-antibody detection for example.

1. GNRs with a LSPR wavelength at 840 nm are functionalized with anti-human IgG, while GNRs with a LSPR at 630 nm are functionalized with anti-rabbit IgG.
2. Microscopy glass slides (3″ × 1″ × 1.0 mm; Fisher Scientific, Pittsburgh, PA) are treated with Piranha and MPTMS solution as described above.
3. 10 μL of antibody-modified GNRs with mixed sizes are dropped onto designated spots on the glass slides and incubated for 2 h. The detection spots are arranged to mimic the layout of a 96 well plate to accommodate an absorption reading by the BioTek plate reader in a high-throughput fashion (Fig. 5).
4. Wash the substrate with water three times and dry it with nitrogen gas.
5. To perform a multiplexed detection, a sample solution (10 μL) of mixed human IgG and rabbit IgG are dropped onto the nanosensing spots and incubated for 30 min until equilibrium.
6. The glass substrate is attached to the bottom of a 96-well plate for absorbance measurement. The UV–Vis absorbance mode is chosen with a scanning range from 400 to 999 nm. As the light source scans the spots from well to well, the corresponding UV–Vis spectra are displayed in the same layout and ready for analysis. Figure 6 is the result of multiplexed biosensing of human and rabbit IgG samples at various concentrations (**Note 7**).

4 Notes

1. All the materials are available from Sigma-Aldrich (St. Louis, MO, USA) unless otherwise noted.
2. The washing steps are crucial for GNR functionalization and immobilization. Three times' washing is optimal to remove the unreacted chemicals and most surfactants. Because CTAB bilayer absorbed on GNR surface could block reactions with gold, it is necessary to decrease its concentration to the critical micelle concentration (CMC) at which GNR is stabilized. Further washing could break the stability of GNR and causes aggregation.
3. ITO-coated glass is chosen because of it conductivity, which makes the GNR on glass observable under scanning electron

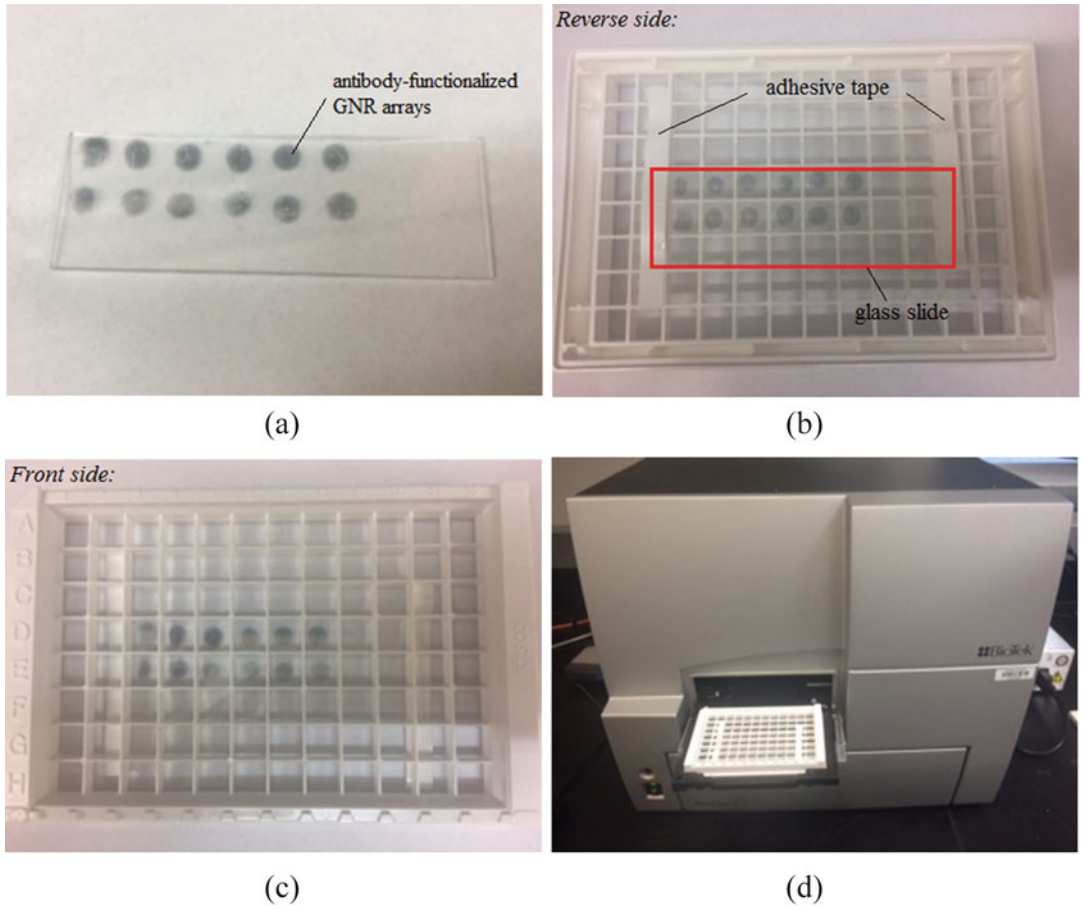

Fig. 5 Representative pictures of (**a**) antibody functionalized GNR array on glass substrates which is expanded to a high-throughput biosensing chip. Each *dark spot*, containing two sizes of functionalized GNRs, works as an individual sensing platform for detecting two antigens simultaneously in one sample. Thus, this biochip can detect 12 samples at one time; (**b**) Reverse side and (**c**) front side of attaching the chip to the bottom of a 96-well plate frame for accommodating the reading on microplate reader (**d**)

microscope (SEM). The ITO coating doesn't influence MPTMS treating.

4. As CTAB is replaced by antibodies, SH-PEG is added 10 min after antibody for stabilizing GNRs.
5. Weakly absorbed (not via covalent bonding) GNR nanoparticles onto the glass can be washed off to ensure a stable and robust biochip [17].
6. The nanorod biochip shows a linear response to the analyte in the range from 10 to 60 nM with high sensitivity of 0.27 nm/nM ($R^2 = 0.99$) for human IgG, which is more than 300% comparison with the reported literature with the sensitivity of 0.0607 nm/nM [17].

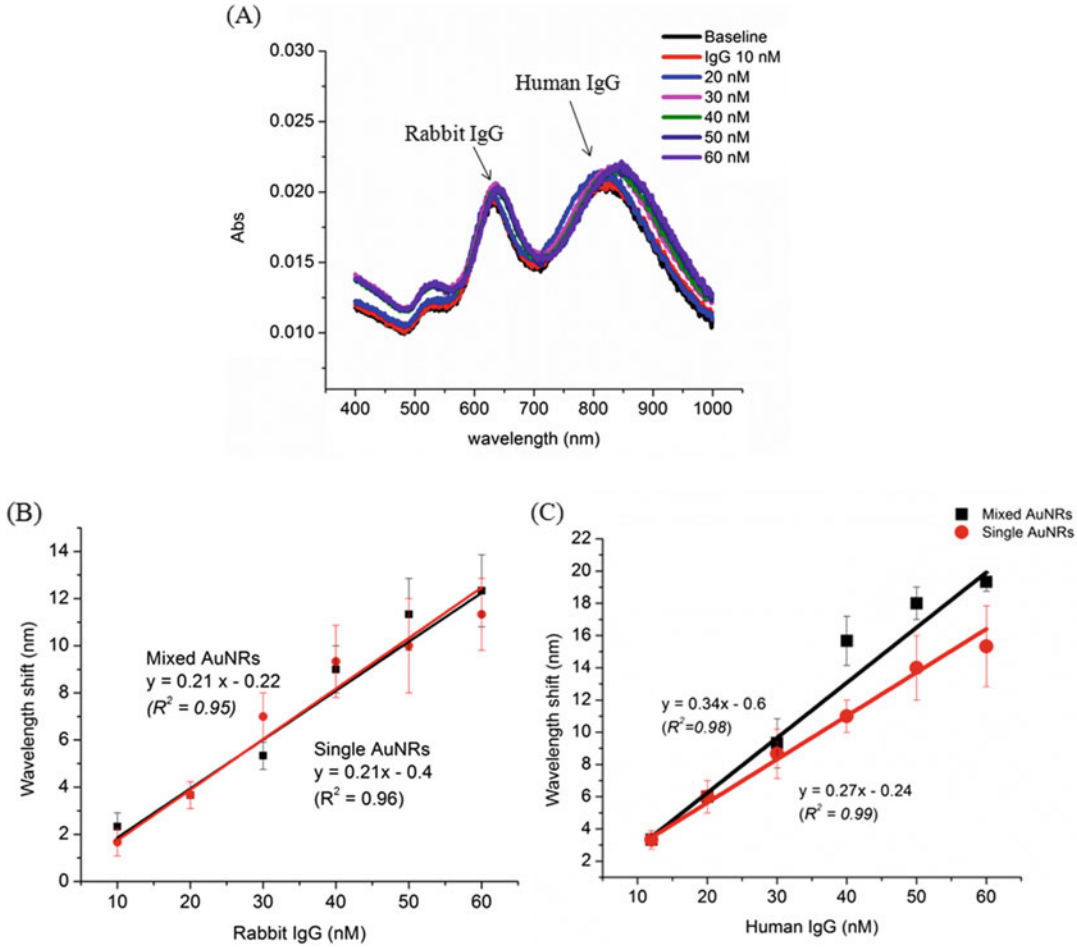

Fig. 6 Multiplexed biosensing of human and rabbit IgG samples at various concentrations. (**a**) UV–Vis spectra of the GNR biochip before and after detection of six various concentrations of mixed IgG. The shorter wavelength around 630 nm is dedicated for rabbit IgG assay, while the longer one around 840 nm for human IgG assay; (**b**) Plotting curve (*black*) of wavelength shift around 630 nm versus the concentration of rabbit IgG; (**c**) Plotting curve (*black*) wavelength shift around 840 nm versus the concentration of human IgG. Both curves suggest that the nanorod chip shows a linear response to the analyte (rabbit or human IgG) in the range from 10 to 60 nM. For comparison, the calibration curves of single GNR based biochip mentioned in Subheading 3.1 are also included (*red*). Interestingly, the multiplexed biosensor has an increased sensitivity than single biosensor for human IgG detection

7. Nonspecific binding studies indicate minimal cross-reactivity of the antibody moieties for high specificity in the multiplexed biosensing. It is observed that the sensitivity is increased as compared to individual detection, especially for longer GNR probes.
8. The biochip achieved by this method demonstrated a random assembly of GNRs on the substrate. Theoretical study has proved that the local electromagnetic field on the tips of a

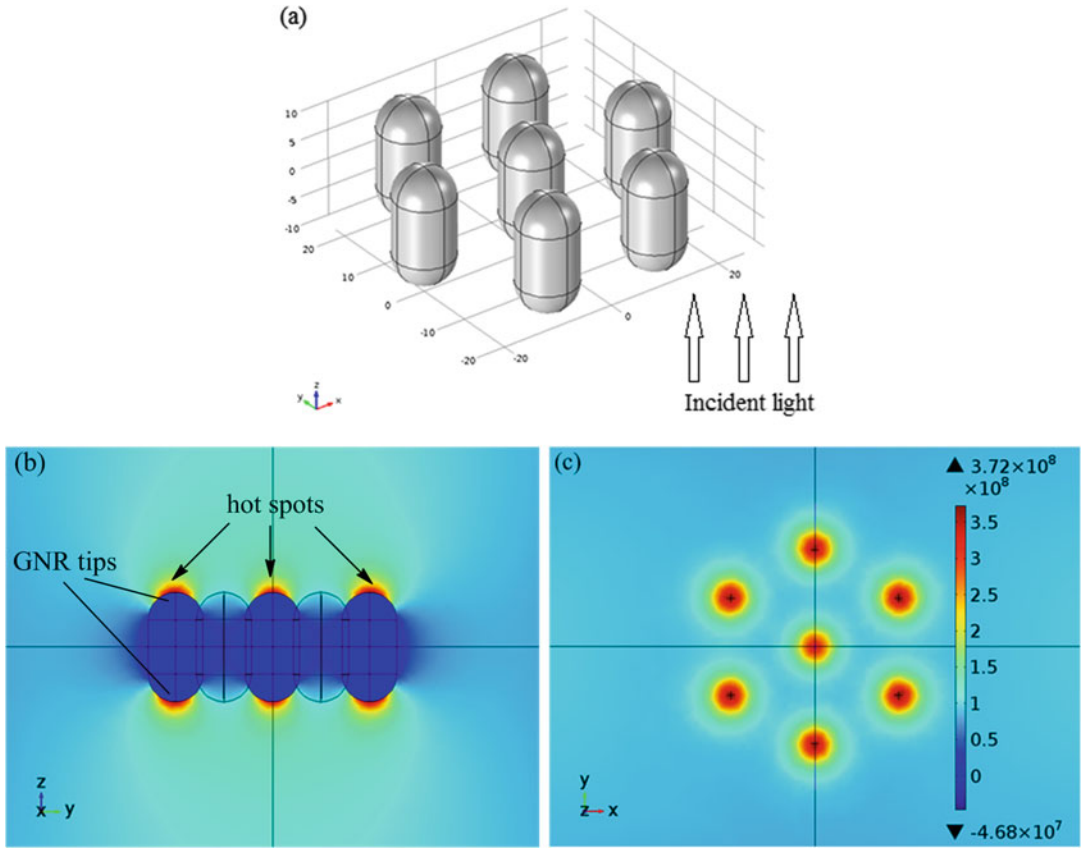

Fig. 7 Local electromagnetic field simulation of a vertical GNR array. (**a**) model of GNR array; (**b**) local field of side view in the cross section along the *y–z* plane; (**c**) local field of the top view along the z direction. The *rainbow bar* shows the intensity. A *redder color* indicates a more intensified local field

nanorod is much stronger than that on the side facets. And the CTAB density of tips is lower than the sides, which ensures a less steric hindrance for the tip modification [18]. For the future perspective, controlling the orientation of the GNR array assembly on the substrate is the current focus. For instance, if GNRs are orderly organized to form a vertically standing array, a large amount of homogeneous hotspots will be created at the GNR surface due to the plasmon coupling effect. Figure 7 is the local electromagnetic field simulation of a vertical nanoarray consisting of seven GNRs using COMSOL 5.0. The incident light with an intensity of 1.0×10^8 V/m propagates along z-direction, passing through the GNR array. The simulation results show that the GNR array exhibit highly uniform and enhanced local field on the tips. This unique property is desired for biomedical applications such as nanoreactor and ultrasensitive SERS sensor [19].

References

1. Giri S, Trewyn BG, Lin VS (2007) Mesoporous silica nanomaterial-based biotechnological and biomedical delivery systems. Nanomedicine (Lond) 2(1):99–111
2. Lee SH, Sung JH, Park TH (2012) Nanomaterial-based biosensor as an emerging tool for biomedical applications. Ann Biomed Eng 40(6):1384–1397
3. Oyelere AK et al (2007) Peptide-conjugated gold nanorods for nuclear targeting. Bioconjug Chem 18(5):1490–1497
4. Chylek P (1986) Absorption and scattering of light by small particles. Appl Opt **25**(18):3166
5. Bennett HS, Rosasco GJ (1978) Resonances in the efficiency factors for absorption: Mie scattering theory. Appl Optics 17(4):491–493
6. Upadhyayula VK (2012) Functionalized gold nanoparticle supported sensory mechanisms applied in detection of chemical and biological threat agents: a review. Anal Chim Acta 715:1–18
7. Yu L, Andriola A (2010) Quantitative gold nanoparticle analysis methods: a review. Talanta 82(3):869–875
8. Dreaden EC et al (2012) The golden age: gold nanoparticles for biomedicine. Chem Soc Rev 41(7):2740–2779
9. Anker JN et al (2008) Biosensing with plasmonic nanosensors. Nat Mater 7(6):442–453
10. Jain PK et al (2006) Calculated absorption and scattering properties of gold nanoparticles of different size, shape, and composition: applications in biological imaging and biomedicine. J Phys Chem B 110(14):7238–7248
11. Chou SF et al (2004) Development of an immunosensor for human ferritin, a nonspecific tumor marker, based on surface plasmon resonance. Biosens Bioelectron 19 (9):999–1005
12. Sim HR, Wark AW, Lee HJ (2010) Attomolar detection of protein biomarkers using biofunctionalized gold nanorods with surface plasmon resonance. Analyst 135(10):2528–2532
13. Ye X et al (2013) Using binary surfactant mixtures to simultaneously improve the dimensional tunability and monodispersity in the seeded growth of gold nanorods. Nano Lett 13(2):765–771
14. Gulati A, Liao H, Hafner JH (2006) Monitoring gold nanorod synthesis by localized surface plasmon resonance. J Phys Chem B 110 (45):22323–22327
15. Wang Y, Tang L (2015) Multiplexed gold nanorod array biochip for multi-sample analysis. Biosens Bioelectron 67:18–24
16. Wang X et al (2015) Gold nanorod biochip functionalization by antibody thiolation. Talanta 136:1–8
17. Wang Y, Tang L (2013) Chemisorption assembly of Au nanorods on mercaptosilanized glass substrate for label-free nanoplasmon biochip. Anal Chim Acta 796:122–129
18. Orendorff CJ, Murphy CJ (2006) Quantitation of metal content in the silver-assisted growth of gold nanorods. J Phys Chem B 110 (9):3990–3994
19. Lim DK et al (2011) Highly uniform and reproducible surface-enhanced Raman scattering from DNA-tailorable nanoparticles with 1-nm interior gap. Nat Nanotechnol 6 (7):452–460